Hindawi Publishing Corporation
Science and Technology of Nuclear Installations
Volume 2012, Article ID 140946, 11 pages
doi:10.1155/2012/140946

Research Article

Solutions without Space-Time Separation for ADS Experiments: Overview on Developments and Applications

B. Merk and V. Glivici-Cotruţă

Helmholtz-Zentrum Dresden-Rossendorf, Institut für Sicherheitsforschung, Postfach 51 01 19, 01314 Dresden, Germany

Correspondence should be addressed to B. Merk, b.merk@hzdr.de

Received 13 December 2011; Accepted 17 March 2012

Academic Editor: Alberto Talamo

The different analytical solutions without space-time separation foreseen for the analysis of ADS experiments are described. The SC3A experiment in the YALINA-Booster facility is described and investigated. For this investigation the very special configuration of YALINA-Booster is analyzed based on HELIOS calculations. The results for the time dependent diffusion and the time dependent P_1 equation are compared with the experimental results for the SC3A configuration. A comparison is given for the deviation between the analytical solution and the experimental results versus the different transport approximations. To improve the representation to the special configuration of YALINA- Booster, a new analytical solution for two energy groups with two sources (central external and boundary source) has been developed starting form the Green's function solution. Very good agreement has been found for these improved analytical solutions.

1. Introduction

Different current and planned experiments (MUSE [1], YALINA [2], GUINEVERE [3]) are designed to study the zero power neutron physical behavior of accelerator-driven systems (ADSs). The detailed analysis of the kinetic space-time behavior of the neutron flux is important for the evaluation of these ADS experiments. Current analysis for all these experiments is based on the standard methods [4]—Sjöstrand method [5] and Slope method [6]—both are based on the point kinetics equations [7]. The point kinetics equations are developed from different approximations to the transport equation. Nevertheless, all these partial differential equations of the transport equation are solved by the separation of space and time to derive the point kinetics equations. The separation of space and time does not provide useful results for cases with strongly space-time dependent external source [8]. In recent years, two big projects have been launched to solve the problem of subcriticality determination in ADS experiments and during ADS operation for the future. In the 6th European Framework program in the integrated project EUROTRANS, the domain 2, ECATS [9] has been dedicated to ADS experiments and the analysis methods for the experiments. In the same time frame, the IAEA has launched the coordinated research project "Analytical and Experimental Benchmark Analyses of Accelerator Driven Systems (ADS)" [10]. Different correction methods based on Monte Carlo Results for the YALINA-Booster system have been derived for the Sjöstrand method as well as for the Slope method in EUROTRANS/ECATS [11, 12]. Good results have been achieved with this correction method for the analysis of the detectors in the thermal zone [13]. Nevertheless, there is still a problem that exists in the fast zone, which is the really important zone, since the follow-up experiment GUINEVERE will be a pure fast system. The results for the analysis of the fast zone of YALINA-Booster are still not convincing, even with the use of correction factors. Good results, but once more only for the thermal and the reflector positions, have been shown in the IAEA CRP by the US American group, especially. These results rely on the use of correction factors from deterministic calculations [14]. The conclusion of the IAEA meeting suggests for further activities, maybe a further CRP among others, the following two topics: "Online Reactivity Monitoring and Control of Sub-critical System"; "Determination of Sub-criticality Level and Uncertainties Analyses" [15].

2. Developed Analytical Solutions for the Analysis of ADS Experiments

To overcome the problems in the analysis of the fast zone in YALINA-Booster and in GUINEVERE as completely fast system, it has been proposed from Helmholtz-Zentrum Dresden-Rossendorf to solve a more elaborate approximation of the transport equation—either the diffusion equation itself (1) or even the time-dependent Telegrapher's equation (2) [16] without separation of space and time. The Telegrapher's equation and the diffusion equation without delayed neutron production are solved completely analytically by using the Green's function method [17, 18]:

$$\frac{1}{v}\frac{\partial\phi}{\partial t} = D\frac{\partial^2\phi}{\partial x^2}\phi - \Sigma_a\phi + S, \tag{1}$$

$$\frac{3D}{v^2}\frac{\partial^2\phi}{\partial t^2} + \frac{1}{v}(1+3D\Sigma_a)\frac{\partial\phi}{\partial t} = D\frac{\partial^2\phi}{\partial x^2}\phi - \Sigma_a\phi + S. \tag{2}$$

Solutions for the Telegrapher's equation have already been provided for a Dirac type pulsed external source [19], for the start-up [20, 21], and for the switch-off [8] of an external source, even with consideration of the delayed neutron production. For the comparison with the experimental results, obtained at the YALINA-Booster facility, a special external source (switch-on followed by a switch-off after a finite time period) has been used for the determination of the analytical solution for the neutron flux [22–25]. The derived solutions for the space-time dependent neutron flux were compared to the detector responses at different locations in the fast area of the YALINA-Booster core [26, 27]. Major results of these comparisons were a good agreement for the spatial distributions during the pulse and only small differences between time-dependent diffusion and time-dependent P_1 transport using identical cross-sections and coefficients [23, 25]. The analysis of the specifics of the YALINA facility forced to extend the analytical solution of the diffusion equation using two energy groups, (3) [28]:

$$\begin{aligned}\frac{1}{v_1}\frac{\partial\phi_1}{\partial t} &= D_1\frac{\partial^2\phi_1}{\partial x^2} - \Sigma_{a1}\phi_1 + \chi_1\left(\nu\Sigma_{f1}\phi_1 + \nu\Sigma_{f2}\phi_2\right)\\ &\quad - \Sigma_{1\to2}\phi_1 + \Sigma_{2\to1}\phi_2 + \chi_{s1}S,\\ \frac{1}{v_2}\frac{\partial\phi_2}{\partial t} &= D_2\frac{\partial^2\phi_2}{\partial x^2} - \Sigma_{a2}\phi_2 + \chi_2\left(\nu\Sigma_{f1}\phi_1 + \nu\Sigma_{f2}\phi_2\right)\\ &\quad + \Sigma_{1\to2}\phi_1 - \Sigma_{2\to1}\phi_2 + \chi_{s2}S.\end{aligned} \tag{3}$$

For a better representation, especially for the experiments in the GUINEVERE facility [3, 29], analytical solutions for one energy group for a two-region system, consisting of a multiplicative core with source and a reflective, only absorbing surrounding (reflector), (4) [30], were calculated:

$$\begin{aligned}\frac{1}{v_1}\frac{\partial\phi_1}{\partial t} &= D_1\frac{\partial^2\phi_1}{\partial x^2} - \Sigma_{a1}\phi_1 + \nu\Sigma_{f1}\phi_1 + S,\\ \frac{1}{v_2}\frac{\partial\phi_2}{\partial t} &= D_2\frac{\partial^2\phi_2}{\partial x^2} - \Sigma_{a1}\phi_2.\end{aligned} \tag{4}$$

For all problems symmetry of the system was assumed and the solutions were derived for a half of the region. Reflective boundary conditions are used in the center of the system, as well as at the outer boundary. In order to connect two regions, continuous neutron flux and neutron current were used for the two-region solution.

The derived Green's functions $G_i(\xi,\tau \mid \xi_0,\tau_0)$ are universal solutions for the solved equation, which are still independent of the definition of the external source in space and time.

The analytical solution for the time-dependent one- and two-group diffusion equation with initial and boundary conditions (1) to (4) is expressed by a double integral in terms of the corresponding Green's functions and the external source, which has to be defined:

$$\Phi_i(\xi,\tau) = \int_{\tau_a}^{\tau}\int_{\xi_0=0}^{R} G_i(\xi,\tau \mid \xi_0,\tau_0)[S(\xi_0,\tau_0)]\,d\xi_0\,d\tau_0, \quad i = I \text{ or } I,\ II. \tag{5}$$

$G_i(\xi,\tau \mid \xi_0,\tau_0)$, $i = I$ or I, II are the Green's functions. A Green's function is a solution for the problem associated with the given problem (one-group diffusion, one-group P_1, two-group diffusion, or two-region one-group diffusion) with the same boundary and initial conditions, in which the nonhomogeneous contribution—in our case the external neutron source $S(\xi_0,\tau_0)$—is replaced by the unit impulse function $\delta(\xi-\xi_0)\delta(\tau-\tau_0)$. In a following step after the determination of the Green's functions, the different kinds of external sources have to be defined. In this way, solutions for a Dirac type pulsed external source [19], for the start-up [20, 21], and for the switch-off [8] of an external source for the time-dependent one-group diffusion and the time-dependent one-group P_1 equation were determined. For the comparison with the YALINA-Booster experiment the external neutron source like it is used in the experiment has to be included and the flux has to be determined by solving (5).

For the described YALINA-Booster experiment with the switch on of an external source followed by a switch off after a finite time step, a Heaviside function **H** was used to model a source function. This Heaviside function is locally concentrated at the center part of the system (see **Figure 1**). In the figure the normalized spatial coordinate points to the front, the normalized time coordinate points to the right, and the source amplitude points upwards. The mathematical definition of the described external source is given by

$$S(\xi_0,\tau_0) \equiv \begin{cases}\dfrac{s(\mathbf{H}(\tau_0-\tau_i)-\mathbf{H}(\tau_0-\tau_a))}{\Delta\xi}, & 0 \le \xi_0 \le \Delta\xi,\\ 0, & \Delta\xi \le \xi_0 \le R.\end{cases} \tag{6}$$

This source was used for the already mentioned comparisons of the one energy group time-dependent diffusion and P_1 solution with the YALINA-Booster experiments [22, 23, 25].

To improve the reproduction of the special experimental conditions with the influences described in Specificity of

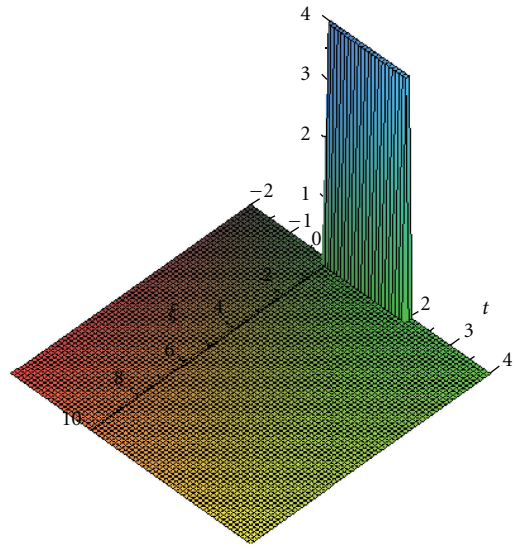

Figure 1: Illustrative sketch of the external neutron source used for the one-group analysis.

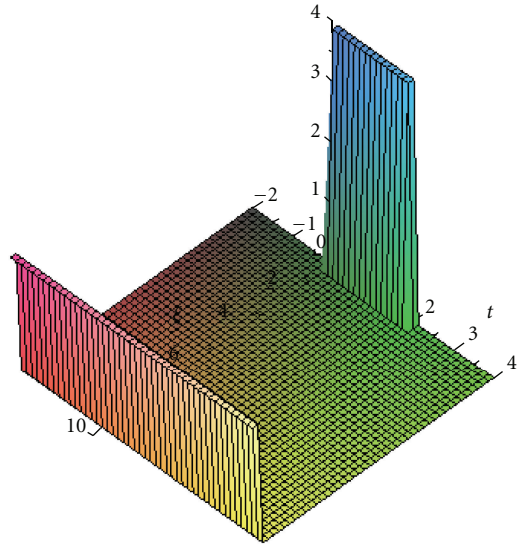

Figure 2: Illustrative sketch for the combination of the space-time dependent external neutron sources for the two-energy group solution.

YALINA-Booster section an additional source has been introduced into the two-group solution to represent the streaming of neutrons from the fast area into the thermal area:

$$S_b(\xi_0, \tau_0) \equiv \begin{cases} 0, & 0 \le \xi_0 \le R - \Delta\xi_b, \\ \dfrac{s_b \mathbf{H}(\tau_0 - \tau_b)}{\Delta\xi_b}, & R - \Delta\xi_b \le \xi_0 \le R. \end{cases} \quad (7)$$

Using the sources, defined in (6) and (7), a combined source is created for the two-energy group analytic solution, as it is sketched in Figure 2. It has to be mentioned that the different contributions of the central source and the boundary source can vary independently for the location and

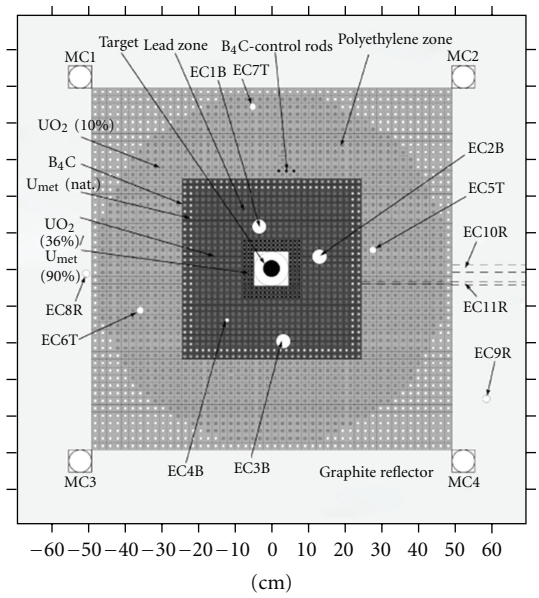

Figure 3: General configuration of the YALINA-Booster core.

for both energy groups. Thus for the experiments the central neutron source in the thermal group is set to zero, since the external source produced via the D-T reaction provides mono-energetic neutrons with 14 MeV. For the time behavior of the boundary source, a simple approximation has been used. The source has been used as constant, since the start-up of the source is not of interest for the analysis and the decay of the neutron flux in the thermal area is significantly slower than in the fast area, due to the strong difference in the neutron generation time.

3. Specificity of YALINA-Booster

The core of the YALINA-Booster facility, located in Belarus, consists of the central target region, surrounded by the region with 90% enriched uranium metal (U_{met} 90%) or 36% enriched uranium oxide (UO_2 36%) rods in a lead matrix. This central region is surrounded by another fast region consisting of a lead matrix with 36% enriched uranium oxide (UO_2 36%) rods. In this region the three experimental channels (EC1B, EC2B, and EC3B) are located (see Figure 3). The fast region is decoupled from the surrounding thermal region by the so-called "valve," consisting of one row of natural uranium metal (U_{met}) rods and one row of boron carbide (B_4C) rods. The thermal region consists of a polyethylene matrix with holes, which are filled either with 10% enriched UO_2 fuel or with air. The core is surrounded by a graphite reflector.

The SC3A configuration (see the HELIOS model in Figure 4) of the YALINA-Booster facility is used for the comparison with the different analytical solutions. The configuration has been modeled in all details in HELIOS for the determination of the one- and two-group cross-section sets [23, 24]. In the SC3A configuration the 90% enriched uranium metal fuel of the inner fast zone is replaced by 36%

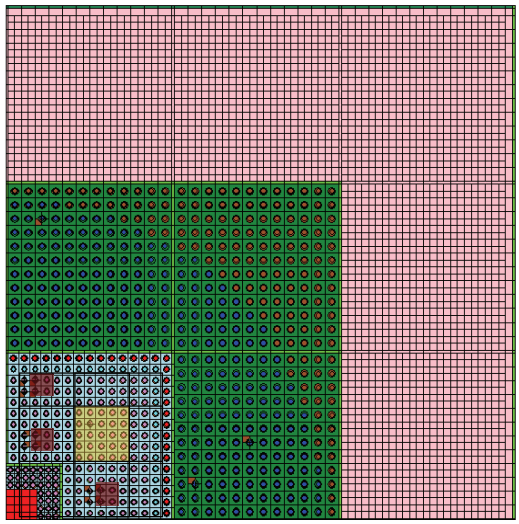

Figure 4: SC3A configuration of the YALINA-Booster core in the HELIOS model for XS preparation.

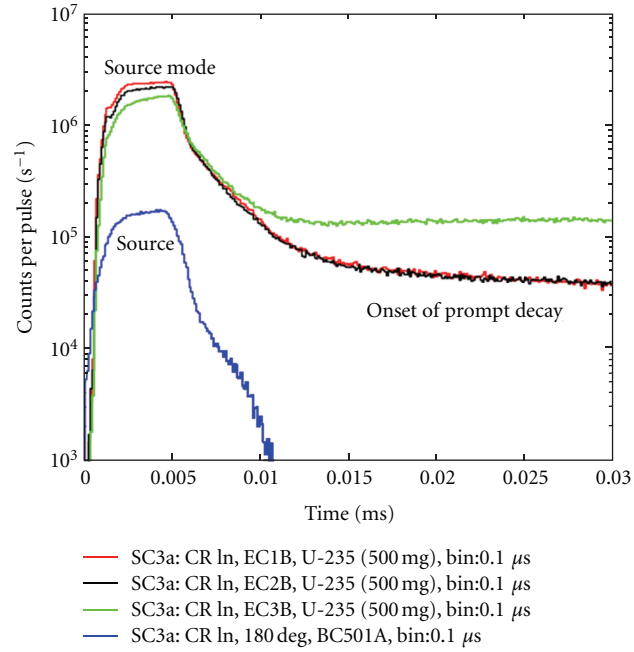

Figure 5: Detector responses in the pulsed neutron source experiment at three different detector positions in the fast area of the SC3A configuration of YALINA-Booster [31].

enriched uranium oxide fuel (tight rows of bright pink rods, which surround the red target zone). The thermal region in green contains the rods in deep blue and the empty positions in brown, respectively. The graphite reflector is shown in rose. The critical 2D HELIOS calculation has been corrected with a leakage term (defined in the HELIOS input by using the input buckling B^2 option) in the third dimension to reach a comparable result to a 3D MCNP calculation for a critical problem [31]. This is used to correct for the really small depth of the YALINA-Booster core ~0.5 m. The k_{eff} of the system with the above-mentioned leakage correction is 0.949090.

For the comparison of the space-time dependent analytical solutions with the real experiment a cross-section set is needed. This cross-section set is calculated with the licensing grade code module HELIOS 1.9 [26]. One-quarter of the YALINA-Booster facility is reproduced in a two-dimensional model in all details in unstructured mesh. The experimental channels are all relocated into the modeled core quarter, but only with the weight of 25%. The microscopic cross-sections are taken from the HELIOS internal library with 190 energy groups. A two-dimensional 190 energy group neutron flux solution is calculated using this library and the above-given geometry with the SC3A material configuration. These neutron flux solutions are used to produce condensed one- and two-group cross-section sets for the yellow overlaid reference element for the YALINA-Booster core in SC3A configuration.

The external source is not taken into account in the HELIOS calculation for the cross-section preparation. The absence of the external source neutrons with 14 MeV from the D-T reaction has the potential to influence the neutron spectrum slightly in the very center of the system. Nevertheless it has to be kept in mind that the amount of external source neutrons is small <5% and the slowing down to "reactor energies" occurs after some collisions in the lead matrix.

The YALINA-Booster facility has a very specific and unusual design. The basic idea was to produce a small fast subcritical reactor experiment for ADS study. The thermal part around the fast system in the lead matrix was introduced to reduce the leakage out of the fast system and to reach an acceptable criticality level in a small facility; the overall core size is below one by one meter. To create the possibility of doing fast system measurements the "valve" was inserted. In theory, the rows consisting of B_4C and natural uranium should prevent the thermal neutrons from the thermal zone from entering the fast zone.

Figure 5 shows the detector responses at the three detector positions in the fast zone of the YALINA-Booster experiment induced by a finite source pulse. The neutron generator was operated in pulse mode. The detector's signals were registered after each pulse. In Figure 5 the histograms of pulses were produced by adding data from all pulses to each other. For a more detailed analysis, the response of the source monitor (blue line) is added to create an insight into the time behavior of the external neutron source. The responses at the two innermost detectors show the expected results, but the response of the outer detector (EC3B in green) shows an unexpected behavior. After the prompt exponential die out of the neutron pulse, all curves should end at approximately the same delayed neutron level. The stable level of the detector response, which is significantly higher at the EC3B even after 0.03 ms, has to be explained. The most convenient explanation for the high detector response after the die out of the prompt pulse in the fast area is the inflow of neutrons from the thermal system. Since the neutron generation time in the thermal area is significantly longer, there is still a high

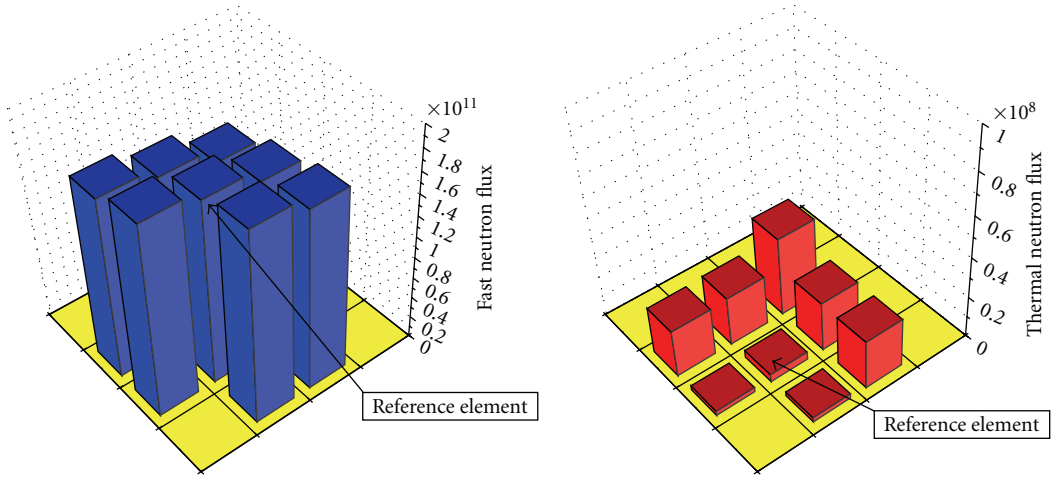

FIGURE 6: Fast neutron flux (a) and thermal neutron flux, (b) in the different relevant fuel elements in the fast part of YALINA-Booster for SC3A.

neutron flux available. The inflow of neutrons from the thermal area should be suppressed by the design using the "valve," the combination of one row of B_4C and one row of natural uranium. The "valve" is more efficient for thermal neutrons, since the absorption coefficient of B-10 for thermal neutrons is high, but fission neutrons can penetrate the "valve" since they are definitely not all well thermalized before they appear at the "valve." A conclusion of the described effect of the insufficient die out of the detector response is that fast fission neutrons born in the thermal area can influence at least the outermost detector in the fast area. Thus, "EC3B is affected by the thermal zone" [31].

A detailed analysis has been performed on the basis of the HELIOS model, developed for the cross-section preparation to explain the unexpected results in the cross-section sets [22] and to confirm the thesis of the inflow of neutrons from the thermal area.

The 190 energy group neutron flux calculated with HELIOS is condensed for the detailed analysis of the spatial neutron flux distributions on the basis of the fuel element-like structures, marked in Figure 4. The relevant fast and the thermal neutron flux (cutoff energy is $6.2506 \cdot 10^{-1}$ eV) distributions are shown in Figure 6. The spatial distribution of the fast neutron flux (Figure 6(a)) shows the expected cosine-like distribution. An influence of the neutrons penetrating through the "valve" is not explicitly visible here. The result for the thermal neutron flux (Figure 6(b)) is in strong contrast to the result for the fast neutron flux. In the fast area the thermal flux has to be very low due to the lead matrix in the fast zone of the YALINA-Booster core. The thermal neutron flux shows a distribution which is neither expected nor typical for a reactor core. In contrast to the cosine distribution of the fast neutron flux, the thermal neutron flux grows exponentially with increasing distance from the center. The thermal neutron flux is the highest in the corner of the fast zone, which is surrounded by the thermal zone on both sides. This kind of distribution can be explained only by the ingress of thermal neutrons from the moderated outer, thermal area through the "valve" into the fast area. The comparison of the thermal neutron flux shows an 18 times higher thermal neutron flux in the corner element compared to the elements in the inner row. This significantly higher thermal neutron flux in the outer fuel elements has strong influence on the production of the cross-section set for all kinds of deterministic calculations for YALINA-Booster. The influence of the thermal neutrons on the cross-section preparation is very strong, since the microscopic cross-section, for example, fission of U-235, is more than hundred times higher than for fast neutrons. The macroscopic production cross-section $\nu\Sigma_f$ is roughly a factor of 3 higher in the corner element than in the elements of the inner row. The effect is only a spectral effect, since the materials in all elements are completely identical. In the standard cross-section preparation a fuel element is calculated in infinite grid, where this spectral effect is lost. Thus an adequate flux weighting of the cross-sections requires a simulation of the full YALINA-Booster core. Due to the strong differences in the thermal flux distribution, the cross-sections for identical material at different positions will vary significantly [22].

4. Comparison with the Experiment

4.1. One Group P_1 and Diffusion Solution. The experimental results, shown in Figure 5, are compared with the developed analytical approximation solutions for the first 0.01 ms on a logarithmic scale for a qualitative comparison in Figure 7. The results for the analytical solution for the different detector positions are given as lines, and the experimental results are given as diamonds in the identical color. This graph already shows one of the major problems. The mathematical representation of the external neutron source by two Heaviside functions is only an approximation of the detected pulse of the external source. In the experiment the external neutron source is created by a D-T reaction in the target

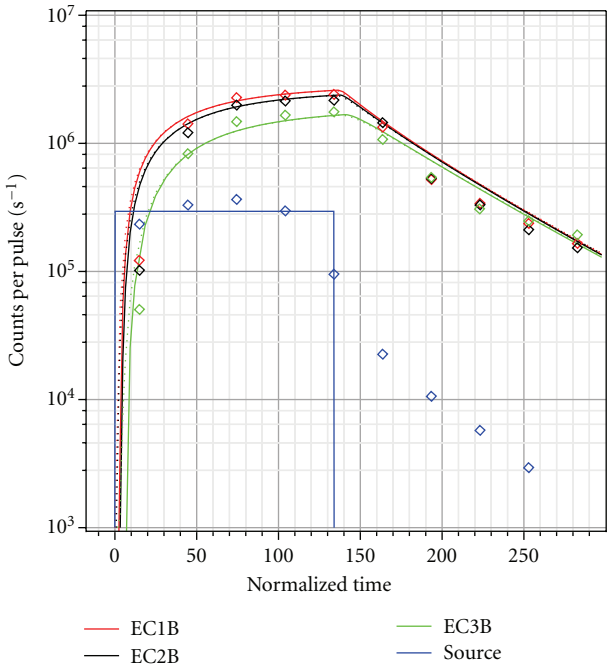

Figure 7: Comparison of the analytical results for the space-time dependent neutron flux (full line—P_1 transport; dotted line—diffusion) with the results for the SC3A experiment at the YALINA-Booster facility on logarithmic scale.

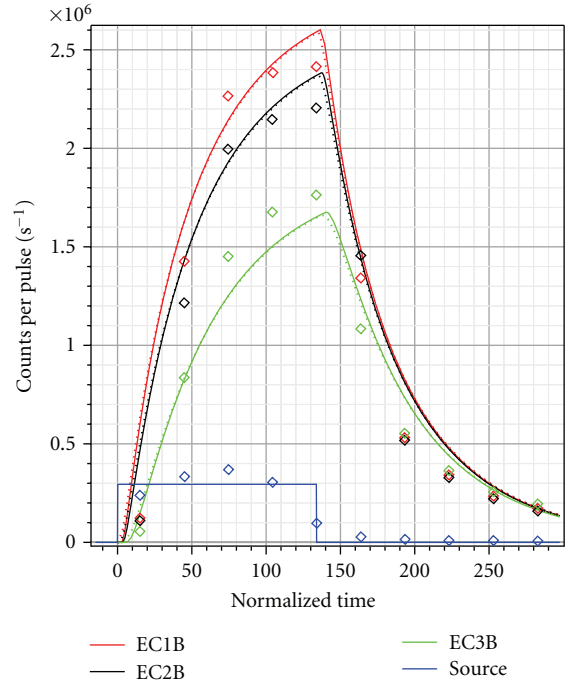

Figure 8: Comparison of the analytical results for the space-time dependent neutron flux (full line—P_1 transport; dotted line—diffusion) with the results for the SC3A experiment at the YALINA-Booster facility on linear scale.

in the center of the YALINA-Booster facility. Unfortunately, switch on as well as switch off of the accelerator, which provides the source with deuterium ions, takes some finite time. With this limitation it is impossible to create really sharp pulse fronts for the external neutron source.

Additionally, the source detector is located in another room with a distance of roughly 4 meters from the target, and the signal, taken from the source monitor, follows another chain of electronics which might have other time properties. Both facts cause some time delay in the source counts compared to the counts in the core. These effects have been taken into account by an estimated time correction of 2 μs for the source.

Nevertheless, a good qualitative agreement between the analytic approximation solutions (P_1 transport—solid line, diffusion—dotted line) and the experimental data is observable. Especially, the spatial distribution in the plateau phase shows a good agreement. This exactly confirms the need and demonstrates the progress of the developed analytic approximation solutions derived without separation of space and time in contrast to the currently used methods based on point kinetics.

The detailed comparison of the developed analytical solutions with the SC3A experimental results at the YALINA-Booster facility on linear scale is shown in Figure 8. It is once more observable that the response of the source detector in the experiment (blue diamonds) does not have the sharp rectangular time behavior like it is used in the development of the analytical solutions. The switch on of the accelerator as well as the switch off of the accelerator cannot be performed in sharp way like it is defined in the mathematical way. This fact causes observable differences in the results for the experiment and the analytical solution on the linear scale. Nevertheless, there is a good agreement between the analytical results with the experimental results. The detector response for the three different detector positions EC1B red, EC2B black, and EC3B green is given at different time points of the experiment by diamonds. The time behavior of the neutron flux at the different positions of the detectors calculated with the analytical solution for the time-dependent P_1 transport solution is given by the full-lines and the results obtained with the analytical solution for the time-dependent diffusion solution with the dotted line: EC1B-red; EC2B-black; EC3B-green. Both analytical solutions show similar behavior with only minor differences in a short time period after the step change in the external source, for the switch on as well as for the switch off. The comparison with the experiment demonstrates that the developed solutions without separation of space and time can reproduce the behavior of the neutron flux at the different detector positions. A small overestimation for the diffusion solution in comparison with the time-dependent P_1 solution is observable in the initiation phase of the transient. The neutron flux grows rapidly after the switch on of the source. After roughly 10 neutron generations the neutron production exceeds due to multiplication of the external neutron source. The calculated neutron flux rises as long as the external source is in operation and would reach a steady state value if the external source would be operated long enough.

The neutron flux decays very rapidly in an exponential manner after the switch off of the external source. The response at the outermost detector is somewhat lower in the calculation. This difference can be once more explained by the ingress of neutrons from the thermal area.

The effect of the fast neutrons, which travel from the thermal into the fast area, is the starting point for the discussion of another important fact. Currently, the analytic approximation is only for one region and one energy group and it has only been applied to the fast area of the system. However, the k_{eff} for the fast area is not known and even a prediction is very problematic, since, on the one hand, the fast area is heavily influenced by the thermal area and the "neutron valve," and on the other hand, the model for the cross-sections is only two-dimensional. These two facts make it nearly impossible to draw a reliable balance between neutron gains and losses for the fast region. Additional problems are caused by the definition of the boundary, since including or excluding of the strong absorber in the "valve" influences the result significantly. A rough estimation of the k_{eff} has given a value around 0.6 for the fast region. This value has finally been used for the calculations with the analytic approximation solutions. This means an analytic solution for two or more regions would be needed to overcome this problem at least partly. Ideally the solution for the thermal area should be additionally expanded to two-energy group. Summing up all mentioned above, we can conclude that a really complicated experiment like YALINA-Booster is not the ideal test case for the development of a new analysis method. A system like Guinevere [3], consisting of only two regions, a pure lead region containing the fuel, and another pure lead region, acting as reflector, will simplify the problem. Nevertheless, at least an analytical solution for two regions would be needed even for this kind of system to determine the real multiplication factor for the system.

4.2. Diffusion versus P_1 Transport. The decision for either the time-dependent P_1 transport equation or the time-dependent diffusion equation for the further development of the analytic approximation solutions is very important. It is required to solve a second-order equation for the development of the analytic approximation solution for the P_1 transport equation. To solve only the time-dependent diffusion equation would lead to a significantly reduced complexity in the solution, since there is only a first-order partial differential equation in time to solve. This reduced complexity offers the possibility to invest more into the spatial or energetic domain of the problem by tracking a system with two or more regions or more than one energy group [28].

It has already been demonstrated that there is a visible deviation between the results for the time-dependent P_1 transport equation and the time-dependent diffusion equation [8, 20, 21]. An evaluation of the deviation Figure 9(a) and the difference Figure 9(b) between the P_1 transport and the diffusion solution for the three different detector positions in YALINA-Booster is shown in Figure 9. The structure of the deviations is identical for all three detector positions. The major deviations occur certainly in the moments directly after the change in the external neutron source. The deviation in the beginning is rather high since the neutron flux used for normalization is comparably low. This deviation dies out after roughly 50 neutron generations for the case of a constant operating source. Following the switch off of the source the deviation rises once more but only to roughly 3% and dies out rapidly during the fade away of the neutron flux. The deviation in the beginning is strongly dependent on the distance from the source. The reason for this deviation is the infinite velocity of a perturbation in the diffusion equation compared to the finite velocity of the spreading of the perturbation in the P_1 transport solution. Due to this fact, the time delay of the reduction of the deviation increases with increasing distance from the external source.

The difference between the time-dependent P_1 result and the time-dependent diffusion result is normalized on an average plateau value of $2 \cdot 10^6$ counts per pulse. This way of evaluation avoids the weighting of the difference by different flux values, which leads, especially in cases of very low neutron flux, to tremendously high deviation. The evaluation of the difference gives a good overview on the quality of the result independent of the actual flux level. The difference during the whole transient is below 4% with peaks at the points of the changes of the external source. Negative difference indicates overestimation by the diffusion result.

Both evaluations show significant differences between the diffusion and the P_1 result, but these differences are low in comparison with the differences between the experimental results and the calculations. The major reasons for the differences between experiment and calculation are the limited representation of the real external source in the experiment and the difficulties to represent the complicated geometric structure (three different regions, three dimensions) of the experimental facility by one energy group, one region, and one-dimensional analytical solution.

The comparison of the time-dependent diffusion and the time-dependent P_1 solutions, both without separation of space and time, shows that already the diffusion solution provides good results for the evaluated finite source pulse experiment. The limitation for the recalculation of the experiment is given by the incomplete representation of the character of the source pulse. Unfortunately, the pulses are not as sharp as it would be needed for a detailed analysis of pulsed source experiments based on a Heaviside step function.

4.3. Two-Energy Group Solution. The results of the analytic approximation solutions for the time-dependent one- and two-group diffusion equation for three different detector positions (EC1B, EC2B, and EC3B) are compared to the detector response in the experiment SC3A in Figure 10. First of all, the same conditions (difference in the temporal source shape, influence of the thermal zone…) exist, but the observed time period has been extended for the analysis of the delayed neutron level. The detector response for the three different detector positions—EC1B (red), EC2B (black), and EC3B (green)—is given once more by diamonds at different time points of the experiment. The time behavior of the neutron flux is calculated in this case with the analytical time-dependent one group diffusion solution (Figure 10(a)). The neutron flux at the different positions of the detector is

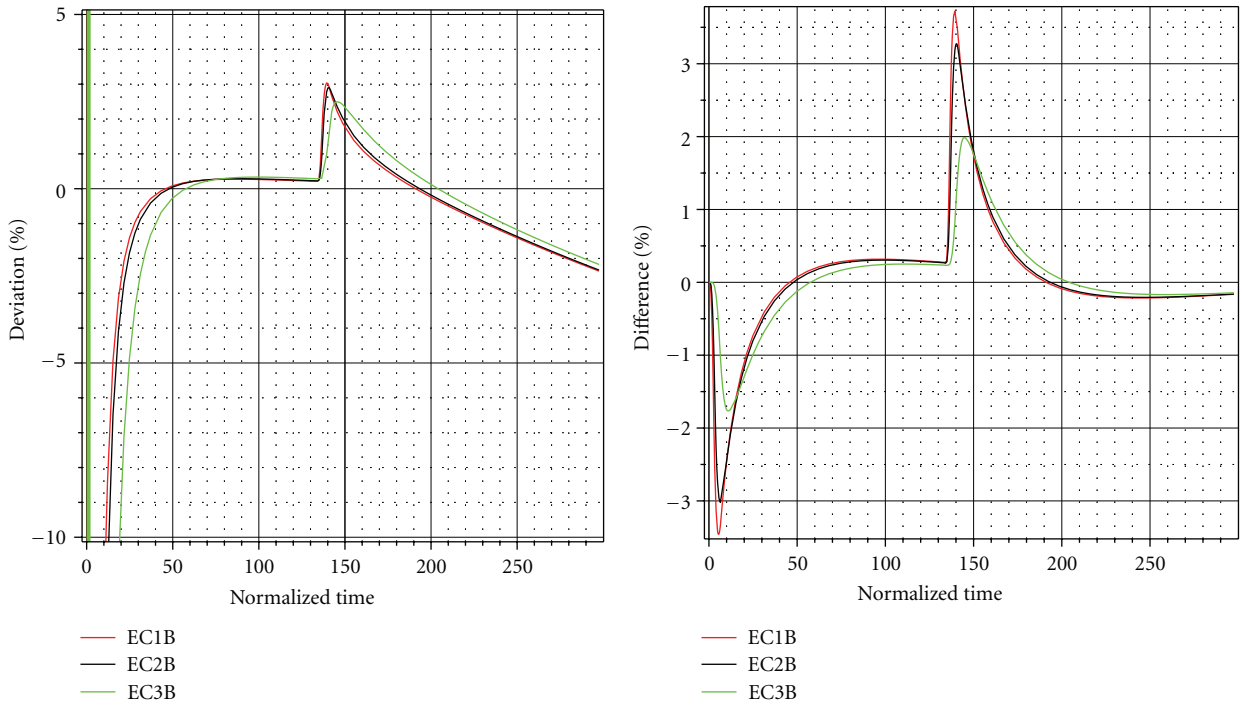

FIGURE 9: Evaluation of the deviation (a) (deviation = $(\Phi_{P1}/\Phi_{\text{diffusion}} - 1) * 100$) and difference, (b) (difference = $\Phi_{P_1} - \Phi_{\text{diffusion}}$) between the time dependent P_1 transport solution and the time dependent diffusion solution at the different detector positions.

given by the full lines: EC1B-red; EC2B-black; EC3B-green. The comparison with the experiment demonstrates that the developed one group solution without space and time separation can reproduce the behavior of the neutron flux at the different positions of the detectors, like it was demonstrated before. The neutron flux decays very rapidly in an exponential manner after the switch off of the external source. Two points show deviations which have to be discussed: first, the response at the outermost detector (green) is somewhat lower in the calculation. This difference can be explained by the location close to the thermal area position. Second, the steady state value of the neutron flux after the switch off of the source is in the experiment significantly higher at the outermost position than in the calculation. This difference indicates once more that there is an influence from the thermal area to the fast area. The neutrons have a significantly longer lifetime in the thermal area; thus there is still a high neutron density available in the thermal area, while the neutron density in the fast area has already decreased significantly. This gradient between the fast and the thermal area leads to the possibility of a neutron inflow to the fast area.

The results of the improved mathematical model, which uses the time-dependent two-group diffusion equation and an adopted source, are shown in the right part of Figure 10. The external source is a combination of the central external source pulse and the time independent boundary source (to reproduce the incoming neutrons from the thermal area), like it is shown in Figure 2. The first significant difference can be seen in the values after the die out of the pulse. The adopted solution shows a very good agreement when the effect of the pulse has died out and the neutrons are still streaming from the thermal area into the fast area due to the significantly slower decay of the prompt flux in the thermal area. Thus the influence of the thermal area on the fast area can be represented with the new model. With the knowledge of having captured this effect, a close look on the peaks is of our interest. In the one group analysis without caring for the neutrons streaming into the fast area, an increased deviation was visible in the outermost detector EC3B. Now this deviation has vanished nearly completely. The representation of all peaks is good and reflects a good reproduction of the spatial distribution of the neutron flux during the pulse. Additionally, the time shape of the pulses at all detector positions has improved and comes closer to the experiment. This improvement can be explained with the use of two different neutron velocities, or neutron generation times, in the two energy group solution, which is simply a better approximation of the real continuous energy flux. The change in the horizontal axis is caused by the different, in the two-group case averaged, neutron generation times.

Overall, the comparison of the results of the different analytic approximations with experimental ones from the YALINA-Booster facility has been successful for the SC3A. The extended solution has only been required due to the very special design of the YALINA-Booster facility.

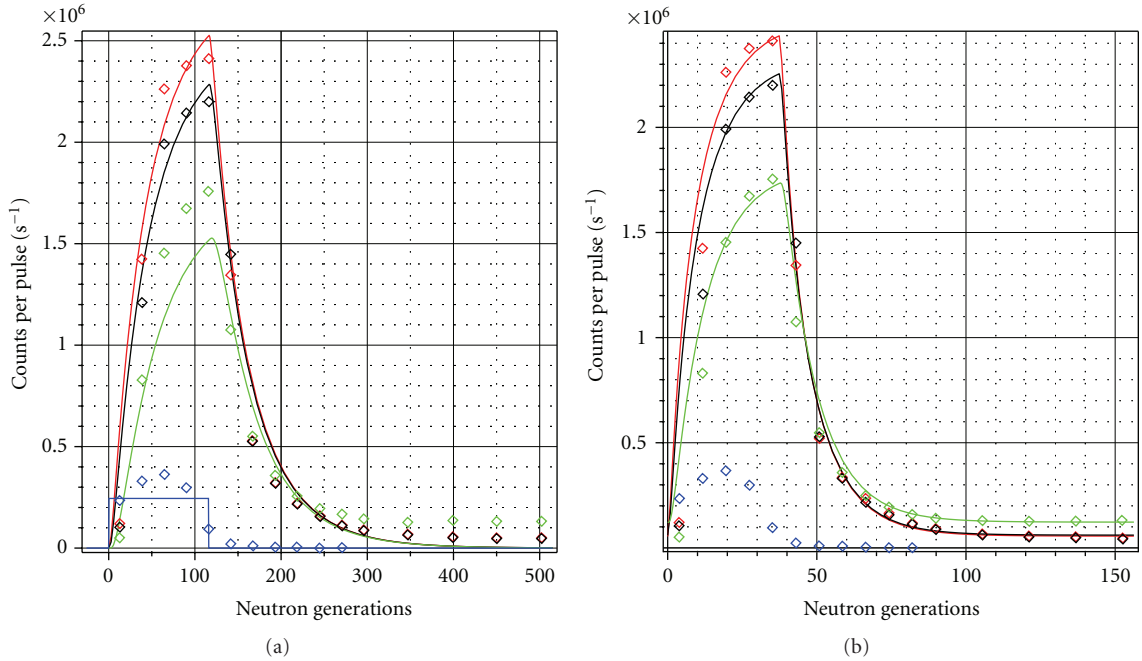

FIGURE 10: Comparison of the analytical results gained with the analytical solution of the time dependent diffusion equation (one-group—(a), two-group—(b)) with the experimental results for the SC3A configuration of the YALINA-Booster facility.

4.4. Two-Spatial Region-Solution. The final idea is to use a solution with two spatial regions, especially for the analysis of the experiments in the GUINEVERE facility [3, 29]. The two-region solution without separation of space and time for the coupled system of a multiplying core with external source and a reflecting surrounding has been derived recently. The flux and the current density are continuous across the interface between two media, and the outer boundaries are reflecting. The exact analytical solution is expressed in terms of a Green's function. The solution is developed by the application of the Laplace transformation [30]. The problems that occur for the one-region solution in YALINA, where the multiplication factor has been calculated only for the region, which is simulated, should be eliminated with this solution for GUIEVERE, where only two regions exist.

The solution will not be applied to YALINA, since two regions would not be sufficient for this complicated configuration. The experiments in the GUINEVERE facility are planned in the beginning of 2012. The successful coupling of the GENEPI accelerator with subcritical VENUS reactor has been announced on October 28, 2011. Early in December an official start-up is scheduled and the first experiments start.

5. Conclusion

A newly developed methodology for reaching a deeper understanding of ADS experiments has been presented as basis for a new method for the analysis of ADS experiments. In the last years at the Helmholtz-Zentrum Dresden-Rossendorf the developed method for the solution of the time-dependent P_1 transport equation, avoiding separation of space and time and based on Green's functions, is promising. Further solutions for the time-dependent diffusion equation for one region and one- and two-energy groups have been used and compared with the YALINA experiments. A special solution for a finite pulse of the localized external neutron source has been developed for all analytical solutions. As an input for the new methodology, a cross-section set has to be created. This is performed with the HELIOS code with a detailed two-dimensional model for the whole core of the YALINA-Booster facility. This detailed two-dimensional transport model has been used to get a deeper insight into the specificity of the YALINA-Booster experimental setup. The detailed analysis of the fast and the thermal neutron flux distribution in the fast area has shown a strong influence of the thermal area on the fast area. This strong influence requires a significantly increased effort for the cross-section preparation. A full model should be used instead of the standard method, which uses a fuel element in reflective surrounding, to catch the effect of the neutron ingress from the thermal to the fast area.

The first comparison of the results of the analytic approximation solutions with experiments from the YALINA-Booster facility has been successful. Good agreement between the experiment and the calculation was obtained in space as well as in time. The comparison of the time-dependent P_1 results with the time-dependent diffusion results has shown that the differences between the modeling and the experiment cause in the case of YALINA significantly stronger differences than the use of different transport approximations. For a better representation of the specifics of the YALINA-Booster setup, a two-energy group solution with

a special arrangement of the sources has been developed which leads to improved results. Since the complicated YALINA-Booster system cannot be represented by a one-region solution the analysis had to be concentrated on the fast zone only. A drawback of this reduction is the limitation of the k_{eff} calculation only to the fast zone. For a prediction of the k_{eff} for the SC3A configuration of the YALINA-Booster facility a calculation for the full system would be essential (at least 3 regions). To overcome this problem for the future experiment GUINEVERE a two region solution has already been developed for the full representation of the GUINEVERE configuration.

Generally, it has to be mentioned that the advantage of the analytical solution over the numerical method lies in the following: the ansalytical solution is an exact solution, which gives dependences on variables; the numerical method is only an approximation to the problem, which causes an inaccuracy, if a large region is considered. Additionally, the numerical method does not give a continuous solution and, in some cases, can be time and resource consuming due to the number of iterations.

Overall, very promising results have been obtained, and a good agreement between the experiment and the calculation has been met in space, as well as in time by using analytical solutions developed without separation of space and time. The flexibility of the analytical solutions for the complicated experimental settings has been demonstrated. Thus, analytical solutions without separation of space and time are a very promising tool to develop a new method for the analysis of ADS experiments.

References

[1] R. Soule, W. Assal, P. Chaussonnet et al., "Neutronic studies in support of accelerator-driven systems: the MUSE experiments in the MASURCA facility," *Nuclear Science and Engineering*, vol. 148, no. 1, pp. 124–152, 2004.

[2] A. I. Kievitskaia et al., "Experimental and theoretical research on transmutation of long-lived fission products and minor actinides in a subcritical assembly driven by a neutron generator," in *Proceedings of the 3rd International Conference on ADTTA*, Praha, Czech Republic, 1999.

[3] H. Aït Abderrahim and P. Baeten, "The GUINEVERE-project at VENUS, project status," in *ECATS Meeting*, Cadarache, France, Januray 2008.

[4] C. M. Persson, P. Seltborg, A. Åhlander et al., "Analysis of reactivity determination methods in the subcritical experiment Yalina," *Nuclear Instruments and Methods in Physics Research, Section A*, vol. 554, no. 1–3, pp. 374–383, 2005.

[5] N. G. Sjöstrand, "Measurements on a subcritical reactor using a pulsed neutron source," *Arkiv för Fysik*, vol. 11, p. 13, 1956.

[6] B. E. Simmons and J. S. King, "A pulsed neutron technique for reactivity determination," *Nuclear Science and Engineering*, vol. 3, p. 595, 1958.

[7] K. Ott and R. Neuhold, *Introductory Nuclear Reactor Dynamics*, American Nuclear Society, La Grange Park, Ill, USA, 1985.

[8] B. Merk and F. P. Weiß, "A three-scale expansion solution for a time-dependent P_1 neutron transport problem with external source," *Nuclear Science and Engineering*, vol. 163, no. 2, pp. 152–174, 2009.

[9] G. Granget et al., "EUROTRANS/ECATS or neutronic experiments for the validation of XT-ADS and EFIT monitoring: status, progress and first assessments," in *OECD Nuclear Energy Agency International Workshop on Technology and Components of Accelerator Driven Systems*, Karlsruhe, Germany, March 2010.

[10] Analytical and Experimental Benchmark Analyses of Accelerator Driven Systems (ADS), http://www.iaea.org/inisnkm/nkm/aws/fnss/crp/crp7.html.

[11] P. Gajda, "Pulsed neutron source measurement in YALINA-subcritical facility," in *Proceedings of the 3rd Environmental Compatible Air Transport System Progress Meeting (ECATS' 10)*, Mol, Belgium, March 2010.

[12] V. Bécares, "Analysis of pulsed neutron source experiments," in *Proceedings of the 3rd Environmental Compatible Air Transport System Progress Meeting (ECATS' 10)*, Mol, Belgium, March 2010.

[13] V. Bécares, D. Villamarín, M. Fernández-Ordóñez, E. M. González-Romero, and Y. Fokov, "Correction methods for reactivity monitoring techniques in Pulsed Neutron Source (PNS) measurements," in *Proceedings of the International Conference on the Physics of Reactors (PHYSOR '10)*, pp. 914–928, Pittsburgh, Pa, USA, May 2010.

[14] Y. Gohar et al., "'Argonne analyses of YALINA-booster', YALINA-thermal, and LEU YALINA-booster," in *IAEA Meeting*, Mumbai, India, February 2010.

[15] Summary of the Technical Meeting on, "'Use of Low Enriched Uranium (LEU Fuel in Accelerator Driven Sub-Critical Assembly (ADS Systems', and 3rd RCM of the CRP on 'Analytical and Experimental Benchmark Analyses of Accelerator Driven Systems'," Mumbai, India, February 2010.

[16] A. M. Weinberg and E. P. Wigner, *The Physical Theory of Neutron Chain Reactors*, University of Chicago Press, Chicago, Ill, USA, 1958.

[17] D. G. Duffy, *Green's Functions with Application*, Chapman & Hall/CRC, 2001.

[18] M. N. Özişik and B. Vick, "Propagation and reflection of thermal waves in a finite medium," *International Journal of Heat and Mass Transfer*, vol. 27, no. 10, pp. 1845–1854, 1984.

[19] B. Merk, "Time dependent analytical approximation solutions for a pulsed source problem: P_1 transport versus diffusion," in *IEEE Nuclear Science Symposium*, Dresden, Germany, 2008.

[20] B. Merk, "An analytical solution for a one dimensional time-dependent neutron transport problem with external source," *Transport Theory and Statistical Physics*, vol. 37, no. 5–7, pp. 535–549, 2008.

[21] B. Merk, "An analytical approximation solution for a time-dependent neutron transport problem with external source and delayed neutron production," *Nuclear Science and Engineering*, vol. 161, no. 1, pp. 49–67, 2009.

[22] B. Merk, V. Glivici-Cotruţă, and F. P. Weiß, "A solution for the telegrapher's equation with external source: application to Yalina—SC3A and SC3B," in *International Conference on the Physics of Reactors (PHYSOR '10)*, pp. 3053–3065, Pittsburgh, Pa, USA, May 2010.

[23] B. Merk, V. Glivici-Cotruta, and F. P. Weiß, "A solution for Telegrapher's equation with external source: development and first application," *Nuovo Cimento della Societa Italiana di Fisica B*, vol. 125, no. 12, pp. 1547–1559, 2010.

[24] B. Merk, V. Glivici-Cotruţă, and F.-P. Weiß, "Application of a two energy group analytical solutions to the YALINA experiment SC3A," in *Proceedings of the International Conference on Mathematics and Computational Methods Applied to Nuclear Science and Engineering (MC '11)*, Rio de Janeiro, Brazil, 2011.

[25] B. Merk, V. Glivici-Cotruţă, and F.-P. Weiß, "A three scale expansion solution for the Telegrapher's equation with external source: development and first application," in *Proceedings of the 21st International Conference on Transport Theory*, Torino, Italy, 2009.
[26] HELIOS Methods, Studsvik Scandpower, 2003.
[27] V. Bécares Palacios et al., "Analysis of PNS measurements at the YALINA-Booster subcritical facility," in *Proceedings of the 2nd EUROTRANS ECATS Progress Meeting*, Aix-en-Provence, France, January 2009.
[28] B. Merk and F. P. Weiß, "A two group analytical approximation solution for an external source problem without separation of space and time," *Annals of Nuclear Energy*, vol. 37, no. 7, pp. 942–952, 2010.
[29] FREYA: Fast Reactor Experiments for hYbrid Applications, http://freya.sckcen.be/en.
[30] V. Glivici-Cotruta and B. Merk, "An analytical solution of the time dependent diffusion equation in a composite slab," submitted to: *Transport Theory and Statistical Physics*.
[31] C. Berglöf, "YALINA-booster: pulsed neutron source characterization," in *Proceedings of the 2nd EUROTRANS ECATS Progress Meeting*, Aix-en-Provence, France, 2009.